Title

Chapter 3 A FRET-based method for monitoring septin polymerization and binding of septin-associated proteins

Authors

Booth, EA
Thorner, J

Publication Date

2016

DOI

10.1016/bs.mcb.2016.03.024

Peer reviewed

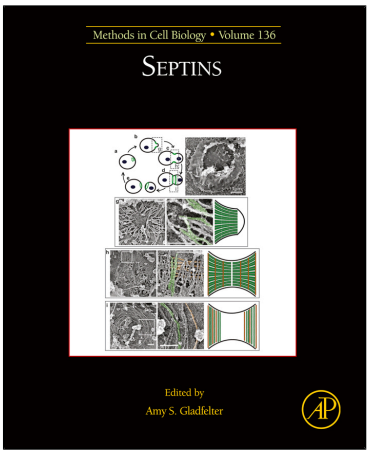

From Booth, E. A., & Thorner, J. (2016). A FRET-based method for monitoring septin polymerization and binding of septin-associated proteins. In A. S. Gladfelter (Ed.), *Septins* (pp. 35–56).
ISBN: 9780128039984

Academic Press

CHAPTER

3 A FRET-based method for monitoring septin polymerization and binding of septin-associated proteins

E.A. Booth[a,b], **J. Thorner**[1,b]

University of California, Berkeley, CA, United States
[1]*Corresponding author: E-mail: jthorner@berkeley.edu*

CHAPTER OUTLINE

Abstract

Much about septin function has been inferred from in vivo studies using mainly genetic methods, and much of what we know about septin organization has been obtained through examination of static structures in vitro primarily by electron microscopy. Deeper

[a]Current address: Grifols Diagnostic Solutions Inc., Emeryville, CA, United States
[b]E.A. Booth ran the experiments shown, analyzed the data, and drafted the manuscript. J. Thorner devised the conceptual approach behind the method described, provided the financial support, and helped prepare the manuscript.

Methods in Cell Biology, Volume 136, ISSN 0091-679X, http://dx.doi.org/10.1016/bs.mcb.2016.03.024

Septins, First Edition, 2016, 35–56

mechanistic insight requires real-time analysis of the dynamics of the assembly of septin-based structures and how other proteins associate with them. We describe here a Förster resonance energy transfer (FRET)-based approach for measuring in vitro the rate and extent of filament formation from septin complexes, binding of other proteins to septin structures, and the apparent affinities of these interactions. FRET is particularly well suited for interrogating protein−protein interactions, especially on a rapid timescale; the spectral change provides an unambiguous indication of whether two elements within the system under study are associating and serves as a molecular-level "ruler" because it is very sensitive to the separation between the donor and acceptor fluorophores over biologically relevant distances ($\leq$10 nm). The necessary procedures involve generation of appropriate cysteine-less and single cysteine-containing septin variants, expression and purification of the heterooctameric complexes containing them, efficient labeling of the purified complexes with desired fluorophores, fluorimetric measurement of FRET, and appropriate safeguards and controls in data acquisition and analysis. Our methods can be used to interrogate the effects of buffer conditions, small molecules, and septin-binding proteins on septin filament assembly or stability; determine the effect of alternative septin subunits, mutational alterations, or posttranslational modifications on assembly; and, delineate the location of septin-binding proteins.

INTRODUCTION

Saccharomyces cerevisiae has a long history of contributing to biological knowledge (Botstein & Fink, 1988) and will continue to be a tractable and facile model organism for interrogating central questions in eukaryotic cell biology for the foreseeable future (Botstein & Fink, 2011). The septins were first discovered by Hartwell and coworkers among the cell division cycle (*cdc*) mutants of this yeast that displayed a failure of cytokinesis at restrictive temperatures (Byers & Goetsch, 1976; Hartwell, 1971; Hartwell, Culotti, Pringle, & Reid, 1974), and *S. cerevisiae* has continued to be indispensable for the study of septin biology (Hall, Russell, & Pringle, 2008). Characterization and cloning of the *CDC3*, *CDC10*, *CDC11*, and *CDC12* genes revealed that their products are related at the sequence level (Field & Kellogg, 1999; Sanders & Field, 1994) and representative of a family of GTP-binding proteins conserved in all eukaryotes (except higher plants) (Nishihama, Onishi, & Pringle, 2011; Pan, Malmberg, & Momany, 2007). Cell staining with specific antibodies demonstrated that these proteins are localized to the neck between a mother and daughter cell (Haarer & Pringle, 1987; Kim, Haarer, & Pringle, 1991). Biochemical studies showed that the four proteins form a stable complex (Farkasovsky, Herter, Voss, & Wittinghofer, 2005; Versele et al., 2004), which electron microscopy (EM) analysis demonstrated was a linear, 32-nm heterooctameric rod with an invariant and well-defined order of subunits: Cdc11-Cdc12-Cdc3-Cdc10-Cdc10-Cdc3-Cdc12-Cdc11 (Bertin et al., 2008) (Fig. 1A). Moreover, under low-salt conditions, these apolar rods could polymerize end-to-end to form long paired filaments in vitro (Bertin et al., 2008, 2010; Farkasovsky et al., 2005). These filaments closely resemble striations at the bud neck in vivo, originally found by EM of grazing

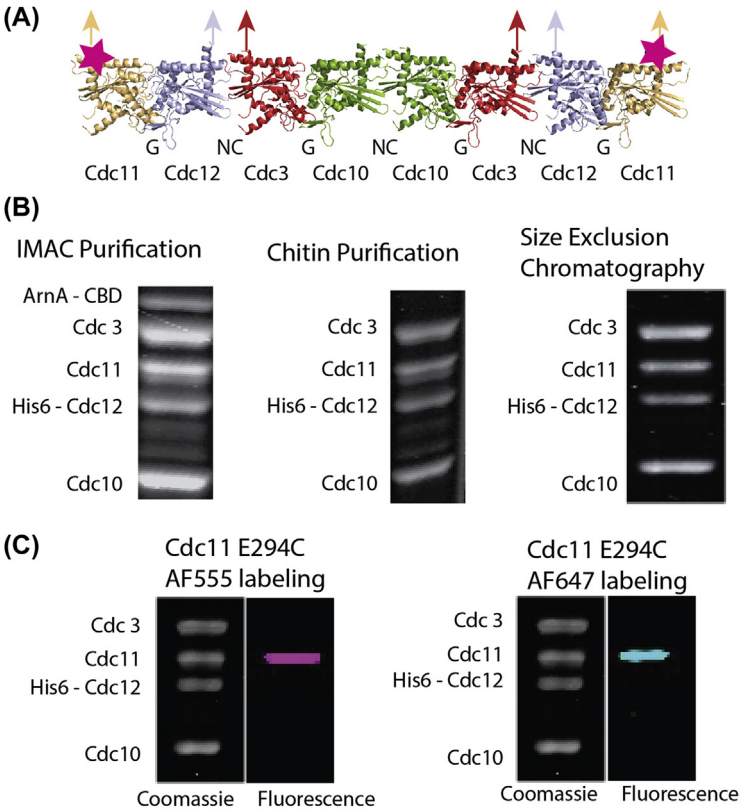

FIGURE 1 Preparation of fluorescently labeled septin heterooctamers.

(A) Model of yeast septin heterooctamer. The *star* indicates the location of the solvent-accessible Cys in Cdc11(E294C) in an otherwise Cys-less heterooctamer. (B) Sodium dodecyl sulfate polyacrylamide gel electrophoresis (SDS-PAGE) gel profiles of the septin-containing fraction from three purification steps: immobilized metal ion affinity chromatography (IMAC) eluate; flow-through from chitin affinity chromatography; and peak fractions from size-exclusion chromatography (SEC). (C) Examples of Cdc11(E294C)-capped and otherwise Cys-less heterooctamers labeled with either AF555-maleimide (donor) or AF647-maleimide (acceptor) fluorophores, as indicated.

thin-sections (Byers & Goetsch, 1976), which other high-resolution techniques have confirmed as septin-based structures (Bertin et al., 2012; Kaplan et al., 2015; Ong, Wloka, Okada, Svitkina, & Bi, 2014). Upon complete sequencing of the *S. cerevisiae* genome (Mewes et al., 1997), three other members of the yeast septin family were recognized: Spr3 (Fares, Goetsch, & Pringle, 1996; Ozsarac, Bhattacharyya, Dawes, & Clancy, 1995) and Spr28 (De Virgilio, DeMarini, & Pringle, 1996), expressed only in *MAT***a**/*MAT*α diploids and only under conditions that trigger meiosis and sporulation (Brar et al., 2012), and Shs1/Sep7, a fifth subunit expressed

in mitotic cells (Carroll, Altman, Schieltz, Yates, & Kellogg, 1998; Mino et al., 1998). Subsequent work has demonstrated that Shs1 is incorporated into septin complexes in place of Cdc11, forming an alternative mitotic heterooctamer: Shs1-Cdc12-Cdc3-Cdc10-Cdc10-Cdc3-Cdc12-Shs1 (Garcia et al., 2011). Similarly, in sporulation-specific septin complexes, Spr28 and Spr3 replace Cdc11 (and Shs1) and Cdc12, respectively, resulting in formation of a meiosis-specific alternative heterooctamer: Spr28-Spr3-Cdc3-Cdc10-Cdc10-Cdc3-Spr3-Spr28 (Garcia et al., 2016).

Unlike the Cdc11-capped rods, the Shs1-capped rods do not polymerize end-on-end in low-salt solution, but associate laterally, forming bundles that interact to form elaborate arcs, rings, and spirals (Garcia et al., 2011). The Spr28-Spr3-capped complexes do not self-associate at all in low-salt solution, but, on the surface of a lipid monolayer containing phosphatidylinositol-4,5-*bis*phosphate (a lipid greatly enriched in the prospore membrane), they do assemble into well-ordered arrays of long paired filaments that display a cross-bridged ultrastructure (Garcia et al., 2016), distinct from the tight pairs assembled by Cdc11-capped rods on the same surface (Bertin et al., 2010).

The human genome encodes 13 septin genes, and many of the corresponding gene products are expressed in a variety of isoforms (Hall & Russell, 2012). However, as in yeast, human septin complexes are also apolar heterooctameric rods, one of the most abundant of which is Sept9-Sept7-Sept6-Sept2-Sept2-Sept6-Sept7-Sept9 (Kim, Froese, Estey, & Trimble, 2011; Sellin, Sandblad, Stenmark, & Gullberg, 2011). In addition to EM analysis to ascertain the composition and order of subunits in septin complexes and to assess their ability to assemble into higher-order structures, views of septins at atomic resolution have been obtained by X-ray crystallography of individual human septins (Macedo et al., 2013; Sirajuddin et al., 2007; Zent, Vetter, & Wittinghofer, 2011), septins from other animals (Zeraik et al., 2014), and a human heterohexameric complex (Sirajuddin et al., 2007, 2009). The latter revealed the alternation of interfaces that join the monomers together into linear heterooctamers. The homodimer at the center associates via an interaction surface dubbed an NC interface because the two subunits associate via contacts provided by residues in and around the N- and C-terminal segments of each monomer, and ~180 degrees away from the NC interface, each monomer of the homodimer interacts with the next subunit in the chain via an interaction surface called a G interface because it involves an *en face* interaction of residues in and around the GTP-binding pocket in each monomer (Fig. 1A). This alternation of interfaces continues out to each end of the rod. Although EM and X-ray analyses provide only snapshots of septin structures, they yield invaluable information for designing biochemical studies to address the underlying dynamics and other mechanistic aspects of septin complex assembly.

Fluorescence microscopy has been applied to study septin assembly in vitro (Bridges et al., 2014; Renz, Johnsson, & Gronemeyer, 2013; Versele et al., 2004), but, due to the diffraction limit of light, such approaches cannot adequately address the mechanistic details of septin assembly. In contrast, fluorescence spectroscopy

has been extremely useful in studying the polymerization and properties of other biopolymers in vitro, especially actin filaments (Cooper, Walker, & Pollard, 1983; Hansen, Zuchero, & Mullins, 2013) and microtubules (Bonne, Heusele, Simon, & Pantaloni, 1985; Sackett, Knutson, & Wolff, 1990). In this regard, unlike assembly of F-actin from monomeric G-actin, or assembly of microtubules from α-β tubulin dimers, formation of higher-order septin-based structures involves the assembly of a building block that has a very elongated geometry (4 × 32 nm). Given the linear organization and extended shape of septin heterooctamers, the method in fluorescence spectrometry that should be ideal for assessing their interactions is Förster resonance energy transfer (FRET) (Foerster, 1946; Knox, 2012; Pietraszewska-Bogiel & Gadella, 2011; Sun, Wallrabe, Seo, & Periasamy, 2011). To assess protein−protein interaction using FRET, one set of molecules is labeled with a donor fluorophore at a defined position that is not rotationally constrained and mixed with another set of molecules labeled with an acceptor fluorophore, also at a defined position that is not rotationally constrained. Donor−acceptor dye pairs are selected that have sufficient spectral overlap between the emission of the donor and the excitation of the acceptor to allow for FRET, but maximize the spectral separation between the excitation wavelengths of the donor and acceptor (Fig. 2A). The sample (Fig. 2B) is illuminated with a wavelength of light that excites the donor fluorophore only, and evidence of FRET is derived by measuring the increase in light produced at the emission wavelength of the acceptor dye (and the commensurate decrease in light at the emission wavelength of the donor) (Fig 2C). If FRET is detected, such a donor−acceptor interaction demonstrates that the two labeled molecules are in close enough proximity to be undergoing a biologically meaningful interaction. Moreover, because FRET efficiency drops off with the sixth power of the distance, it is very sensitive to, and can thus be used to estimate the separation between, the donor and acceptor fluorophores in the range of 1−10 nm. Finally, FRET allows for rapid measurements under conditions that are readily accessible to manipulation of the buffer composition, temperature, and other parameters.

We have established a FRET-based method for monitoring septin−septin interaction and demonstrated its importance and utility as a method for studying septin assembly (Booth, Vane, Dovala, & Thorner, 2015). For example, in the case of Cdc11-capped mitotic heterooctamers, we anticipated that a batch of purified rods (Fig. 1B) labeled with a donor dye on Cdc11 (Fig. 1C) should display readily detectable FRET when mixed with another batch of rods that have been labeled with an acceptor dye on Cdc11 (Fig. 1C) because it has been amply demonstrated that these rods polymerize end-to-end by the formation of an NC interface between the terminal Cdc11 subunits in adjacent rods (Fig. 2B), and we indeed observed the expected spectral signatures of robust FRET (Fig. 2C−E). It is the intention of this article to provide detailed step-by-step information about the specific methods that we used to prepare and label septin subunits and to conduct the fluorimetric measurements necessary to obtain FRET spectra, as well as additional information about the mathematical techniques we employed to analyze and evaluate the data we collected. To accomplish these goals, we have divided this chapter into two parts. To make the

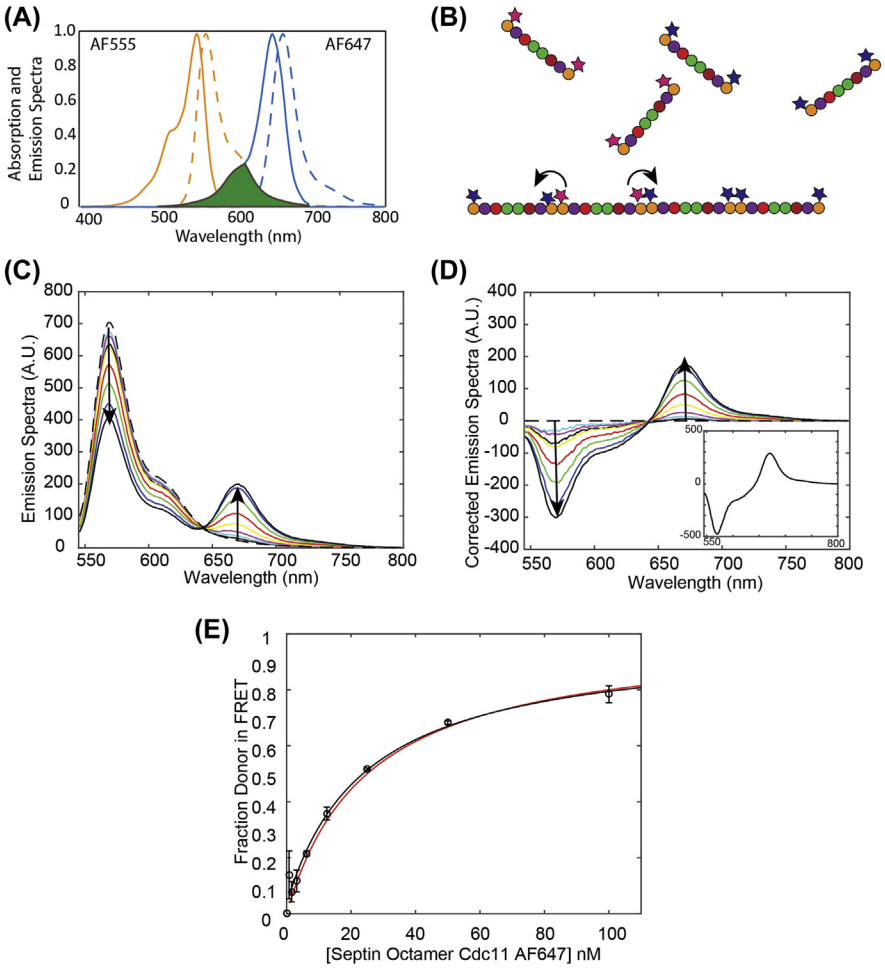

FIGURE 2 Analysis of Förster resonance energy transfer (FRET) fluorescence spectra using the principal component analysis (PCA) method.

(A) Absorbance (*solid line*) and emission (*dotted line*) spectra for donor AF555 (orange (light gray in print versions)) and acceptor AF647 (blue (gray in print versions)) with the donor emission and acceptor excitation spectral overlap highlighted (green (dark gray in print versions)). (B) Stochastically, half of the junctions formed during end-on-end assembly of filaments from a 50:50 mixture of donor dye–labeled heterooctamers and acceptor dye–labeled heterooctamers should display FRET (*arrowheads*). (C) FRET spectra showing the decrease in the donor emission (*left arrow*) and increase in acceptor emission (*right arrow*) as an increasing concentration of acceptor-labeled heterooctamers was added to a fixed concentration (25 nM) of donor dye–labeled heterooctamers. (D) The FRET spectra shown in (C) corrected for the donor-only and the acceptor-only spectra, isolating the changes in donor and acceptor emission, demonstrating that these changes are indeed the principal components (inset) responsible for the FRET observed. (E) The data from the titration experiment in (C) replotted as a binding curve (*black circles*; error bars representing SEM), yielding a measured $K_d = 24.28 \pm 13.65$ nM. Modeling assuming that association of the heterooctamers is completely stochastic predicts the accompanying curve for the FRET change (*red (light gray in print versions) line*).

subsequent experiments more clearly interpretable, the first section focuses on generation of the Cys-containing variants necessary for site-specific dye labeling, purification of recombinant septin complexes suitable for labeling, and the conditions required for efficient fluorophore conjugation. The second section focuses on experimental setup, data collection, and techniques for analyzing the FRET spectra that we found were particularly useful for the septin system. Specific commentary is provided on those features of our methods that need to be considered in reagent preparation, experimental design, and data analysis. The methodology presented here has important implications for further understanding how septins behave as a polymeric system, what conditions directly affect the system, and the potential to assess the roles of different septin-binding partners.

1. PROTEIN PREPARATION AND LABELING

Expression of recombinant proteins in the bacterium *Escherichia coli* is a well-characterized and widely employed procedure that provides a reliable platform for rapid and large-scale production of proteins, as well as an experimentally accessible system for introducing and examining the effects of point mutations, truncations, and/or other perturbations in the proteins being expressed (Duong-Ly & Gabelli, 2014; Kim, Babnigg, et al., 2011). Stable multi-subunit complexes of septins from both *S. cerevisiae* (Bertin et al., 2008; Farkasovsky et al., 2005; Garcia et al., 2011, 2016; Versele et al., 2004) and from humans (Sirajuddin et al., 2007, 2009) have been expressed and purified from *E. coli*. However, the usual caveats for expression of eukaryotic proteins in prokaryotic cells exist, including potential effects of codon usage, lack of appropriate chaperones, and/or absence of a potentially relevant post-translational modification. Likewise, one needs to carefully consider the degree of purity of the final product that needs to be achieved. In the case of use of the final purified product for in vitro FRET experiments, near-homogeneity is essential because contaminants can often contain Cys residues, which will interfere with labeling by maleimide-derivatized dyes (see Section 1.2). To deal with these issues, we have optimized our expression, purification, and labeling methods, as described in the following sections.

1.1 EXPRESSION AND PURIFICATION OF SINGLE-CYS YEAST SEPTIN HETEROOCTAMERS

Yeast septin heterooctamers have been expressed successfully in *E. coli* strains BL21 (DE3), or BL21-CodonPlus(DE3)-RIL, which carries extra copies of the *E. coli argU*, *ileY*, and *leuW* tRNA genes to enhance expression of proteins containing rare codons (Agilent Technologies, Inc.; originally developed by Stratagene, Inc.). We found early on that Cdc12 is the limiting subunit for assembly of stoichiometric complexes of the mitotic septins (Versele et al., 2004); therefore, we coexpress $(His)_6$Cdc12 and untagged versions of Cdc3, Cdc10, and Cdc11 (or Shs1)

and use immobilized metal ion affinity chromatography (IMAC) on Ni^{2+}-loaded nitrilotriacetate (NTA)-agarose beads as our first purification step. However, it has been demonstrated that there are a number of endogenous *E. coli* proteins (ArnA, GlmS, SlyD, and YadF/Can) that are routinely recovered as major contaminants in purifications that utilize IMAC (Bolanos-Garcia & Davies, 2006). For this reason, we use as our production strain *E. coli* NiCo21 (DE3) (New England BioLabs, Inc.) because it has been engineered to prevent recovery of these endogenous *E. coli* Ni^{2+}-bead-binding contaminants. In *E. coli* NiCo21 (DE3), GlmS is mutated to prevent its metal ion binding and ArnA, SlyD, and YadF/Can (essential gene products) are tagged with a chitin-binding domain (CBD) to enable their efficient removal via subsequent chitin affinity chromatography (Robichon, Luo, Causey, Benner, & Samuelson, 2011).

Removal of contaminating *E. coli* ArnA (formerly PmrI) is especially important for preparing recombinant yeast septin complexes of high purity. ArnA is a 70 kDa polypeptide that self-assembles into two stacked trimers (Gatzeva-Topalova, May, & Sousa, 2005), and it is clearly enriched in the septin-containing eluate of a Ni^{2+}-NTA column (Fig. 1B). This globular homohexamer has a molecular mass (420 kDa) somewhat larger than that calculated for the Cdc11-Cdc12-Cdc3-Cdc10-Cdc10-Cdc3-Cdc12-Cdc11 complex (383 kDa). However, upon size-exclusion chromatography (SEC), ordinarily a very effective purification step for a complex as large as the septin heterooctamer, the septin complex coelutes to a significant degree with ArnA, if it is present, because the elongated rod shape of the septin complex causes it to elute with a larger apparent size and, thus, not be well resolved from the ArnA homohexamer. Moreover, each ArnA polypeptide contains 11 cysteine (Cys) residues, which upon maleimide-dye labeling would generate a species that would interfere with fluorimetric analysis to an unacceptable degree. Hence, removal of ArnA-CBD by chitin affinity chromatography prior to SEC is essential (Fig. 1B).

Pairs of individual septin subunits were coexpressed from each of two DUET vectors (EMD Millipore) with compatible origins of replication under selection for both the ampicillin and chloramphenicol resistance cassettes essentially as described in detail previously (Bertin et al., 2008; Versele et al., 2004), but, for the reasons stated immediately above, in *E. coli* NiCo21 (DE3). Bacterial cultures were grown in 2.8 L baffled Fernbach flasks to a density of $A_{600\ nm} = 0.8-1.0$ at 37°C, at which time the temperature was reduced to 16°C and the cells were induced with isopropyl-β-thiogalactoside (IPTG, 0.5 mM final concentration) and allowed to grow overnight at 16°C with shaking at 225 rpm. The cells were collected by centrifugation and resuspended in ice-cold lysis buffer [300 mM KCl, 2 mM $MgCl_2$, 40 μM GDP, 0.1% monothioglycerol, 0.5% Tween-20, 12% glycerol, 20 mM imidazole, 50 mM Tris−HCl (final pH 8.0), 0.2 mg/mL lysozyme with protease inhibitor mix (cOmplete EDTA-free, Roche)].

Cells were ruptured via sonic irradiation with a Branson Cell Disrupter (Model W185D) while held on ice; specifically, the cells underwent 15-s pulses of sonic irradiation followed by 15-s cooling periods, repeated a total of six times. (In the past, we have used alternate methods for breaking the bacterial cells, such as lysis by passage

through a French pressure cell and successfully obtained intact stoichiometric septin complexes.) The resulting lysate was then clarified by centrifugation at 10,000 × g for 30 min at 4°C. The clarified lysate was subjected to IMAC purification using Ni^{2+}-NTA agarose beads (Qiagen). As mentioned previously, in the plasmid constructs used for expression, only Cdc12 carries an N-terminal $(His)_6$ tag, and the remaining subunits are the native proteins. The lysate was incubated with the resin in an Econo-Column (BioRad) with agitation on a rocker platform for 30 min to 1 h at 4°C. The column was affixed upright and the flow-through collected, and the resin then was washed with 5 column volumes of high-salt wash buffer [300 mM KCl, 20 mM imidazole, 50 mM Tris−HCl (final pH 8.0)], followed by elution with 5 column volumes of high-salt elution buffer [300 mM KCl, 500 mM imidazole, 50 mM Tris−HCl (final pH 8.0)]. Fractions containing the bulk of the septins [as determined by sodium dodecyl sulfate polyacrylamide gel electrophoresis (SDS-PAGE)] were combined in preparation for chitin affinity chromatography.

As discussed previously, when using *E. coli* NiCo21 (DE3) as the production strain, chitin affinity chromatography permits the removal of endogenous *E. coli* proteins that are major contaminants in the eluate of an IMAC column. For this reason, the combined eluate from the IMAC purification step (approximately 6−8 mL) was incubated in a fresh Econo-Column (BioRad) containing ~1 mL of chitin resin (NEB) with agitation on a rocker platform for 15−30 min at 4°C. The column was affixed upright and the flow-through collected, and then the column was washed with an additional column volume of elution buffer [300 mM KCl, 500 mM imidazole, 50 mM Tris−HCl (final pH 8.0)] to collect all of the unbound protein, including the septin complexes. The ArnA-CBD (SlyD-CBD and YadF/Can-CBD) present in the Ni^{2+}-NTA fraction is absent in the eluate of the chitin affinity column (Fig. 1B).

The eluate of the chitin affinity resin was then subjected to SEC on a Superdex-200 HiLoad 16/600 (16 mm × 60 cm) column (GE Healthcare) at 4°C. Prior to use, the SEC column was preequilibrated with 2 column volumes of septin buffer [300 mM KCl, 50 mM Tris−HCl (final pH 8.0)]. Fractions were collected using an ÄKTA FPLC system (GE Healthcare), and the protein content of each fraction was assessed by SDS-PAGE and staining with Coomassie Blue dye. Those fractions that contained pure septin complexes and stoichiometric ratios of the subunits were pooled and used immediately for maleimide-dye labeling (Fig. 1C). If any lingering contaminants are present, anion exchange chromatography can be used as an additional purification step, as described earlier (Bertin et al., 2008).

1.2 SINGLE-CYS SEPTIN SUBUNITS AND DYE LABELING BY MALEIMIDE CHEMISTRY

Fortuitously, none of the *S. cerevisiae* septin subunits expressed in mitotic cells contain more than three Cys: Cdc3 (C124 C253 C279), Cdc10 (C266), Cdc11 (C43 C137 C138), Cdc12 (C40 C278), and Shs1 (C29 C148). We have demonstrated in detail elsewhere (de Val et al., 2013) that each of these Cys can be replaced by

Ala, Ser, Val, or Phe [Cdc3 (C124V C253V C279V), Cdc10 (C266S), Cdc11 (C43F C137A C138A), $(His)_6$-Cdc12 (C40A C278S), and Shs1(C29V C148S)] and that each resulting Cys-less subunit is able to support yeast cell viability in the absence of the corresponding wild-type subunit. Moreover, we found that when Cys-less Cdc10, Cdc11, and Cdc12 were chromosomally expressed and Cys-less Cdc3 was overexpressed from a plasmid, cells were able to grow normally at 30°C and that corresponding recombinant heterooctameric complexes were indistinguishable in their in vitro assembly properties from those produced from their wild-type counterparts (de Val et al., 2013). Finally, and most importantly for the application of FRET to study septins, we found that heterooctamers in which a single Cys had been reintroduced at a desired position were stable and able to form filaments in vitro as visualized by EM (de Val et al., 2013).

To enable our FRET approach, into each Cys-less subunit, standard site-directed mutagenesis techniques were used to install a single Cys in place of the residue that, on the basis of sequence alignments and modeling (McMurray & Thorner, 2008) against the crystal structure of the human septin complex (Sirajuddin et al., 2007), should occupy a solvent-exposed position at the base of the predicted C-terminal extension (CTE) in Cdc11, Cdc12, Cdc3, and Shs1, and near the carboxyl terminus of Cdc10 (which is the only mitotic septin that lacks a CTE), yielding Cdc11(E294C), Cdc12(L310C), Cdc3(S407C), Shs1(E344C), and Cdc10(R298C) (Booth et al., 2015; de Val et al., 2013). By placing a single Cys at this location, it should be sufficiently accessible for efficient dye labeling, and the resulting conjugated fluorophore would be close to the globular GTP-binding domain and relatively free from constraints on its rotation. Hence, recombinant septin complexes containing one of these single-Cys-less subunits and three other Cys-less subunits were expressed and purified by the procedures described previously.

Prior to its maleimide-dye labeling, the protein concentration of a purified, recombinant single-Cys-containing heterooctamer was determined using the bicinchoninic acid method (BCA protein assay kit; Pierce). To maximize the thiol content of the sample, it was treated with a 10-fold molar excess of the reducing agent *tris*-(2-carboxyethyl)phosphine (TCEP) for 10 min at room temperature. To remove the excess TCEP and exchange the reduced protein into dye labeling buffer [300 mM KCl, 50 mM Tris−HCl (final pH 7.0)], the sample was passed through a Sephadex G25 desalting column (8.3 mL; PD-10 column, GE Healthcare). The sample was then incubated overnight at 4°C with a fivefold molar excess of the desired maleimide-derivatized dye—Alexa Fluor 555 (AF555) or Alexa Fluor 647 (AF647). Dye labeling was quenched by addition of a 10-fold molar excess of dithiothreitol (DTT) for 10 min at room temperature. At this point, IMAC was used both to concentrate the dye-labeled protein and to remove the excess quenched dye. The sample was manually loaded onto a 1 mL HisTrap HP column (GE Healthcare) preequilibrated with 5 column volumes of wash buffer [300 mM KCl, 50 mM Tris−HCl (final pH 8.0), 20 mM imidazole]. The resin was then washed with 5 column volumes of wash buffer followed by elution with 5 column volumes of elution buffer [300 mM KCl, 50 mM Tris−HCl (final pH 8.0), 500 mM imidazole]. During the

elution a clear band of labeled protein comes off the column and enrichment of the protein can readily be achieved by manual collection instead of automated collection. Concentration of the protein using this method is important, as septin complexes tend to stick to the surface of the filters in the spin columns typically used to reduce the volume of protein-containing solutions. To decrease the imidazole concentration, the dye-labeled protein was dialyzed overnight at 4°C against septin buffer [300 mM KCl, 50 mM Tris−HCl (final pH 8.0)] in a Slide-a-lyzer cassette (Thermo Fisher Scientific) with a 10 kDa molecular weight cutoff.

At this point, both the dye concentration and the protein concentration (corrected for contribution from the dye) must be determined as accurately as possible because this information is necessary for analysis of the FRET data. We utilized Beer's law to determine spectroscopically the molarity of the conjugated fluorophore present (using a P-330 Nanophotometer, Implen) and utilized the BCA reaction (corrected for contribution from the dye) to determine the protein concentration present. These two pieces of information are used to calculate the efficiency of labeling (ie, the number of moles of fluorophore per mole of labeled subunit). In addition, we always confirm that the correct septin subunit has been labeled by resolving the purified dye-labeled septin complexes by SDS-PAGE, visualizing all the subunits by Coomassie Blue dye staining and detecting the fluorophore present by scanning the same gel using a Typhoon Trio Variable Mode Imager equipped for fluorescence (GE Healthcare). Examples of such an analysis for purified single-Cys septin complexes capped with Cdc11(E294C) that were labeled either with the donor fluorophore AF555 (*left*) or with the acceptor fluorophore AF647 (*right*) are shown in Fig. 1C.

1.3 SELECTION OF FLUOROPHORES FOR FÖRSTER RESONANCE ENERGY TRANSFER ANALYSIS

FRET is a physical process occurring between two light-absorbing and light-emitting molecules. FRET between fluorophores requires that (1) the emission spectrum of the donor must overlap the excitation spectrum of the acceptor; (2) the transition dipoles of the two molecules be in a favorable (i.e, nonorthogonal) orientation; and (3) the two molecules be in very close spatial proximity (Foerster, 1946; Knox, 2012; Pietraszewska-Bogiel & Gadella, 2011; Sun et al., 2011). The hallmark of FRET is that when the sample is illuminated at the excitation wavelength of the donor, emission from the acceptor is detected and occurs concomitant with a decrease in the emission of the donor. The 50% transfer distance (R_0) is the distance at which energy transfer is 50% efficient, and the magnitude of R_0 is dependent on the spectral properties of the donor and acceptor dyes, as well as on the refractive index of the medium in which the proteins are suspended. Depending on the pairs of donor and acceptor dyes chosen, the value of R_0 can vary from a few to tens of nanometers; therefore, given the properties of any given experimental system, it is possible to select a pair of donor and acceptor dyes that should have the most favorable R_0 value. Additional considerations for choosing fluorophores include photostability, fluorescence

lifetime, quantum yield, and brightness (Lakowicz, 2006). Eq. (1) shows the relationship between distance and the efficiency of transfer by FRET, where r represents distance, R_0 is the known 50% transfer distance for the fluorophore pair used, and E is the efficiency of transfer. Experimentally, E can be determined by taking the ratio of the intensity of the donor in the presence of the acceptor (F_{DA}) over the intensity of a donor-only sample (F_D); this information, along with the known R_0 value, allows the determination of r and, thus use of FRET as a "spectroscopic ruler." Briefly, we chose the AF555 and AF647 fluorophores because prior studies had demonstrated that they shared good spectral overlap (Fig. 2A) and had an R_0 of 5.1 nm. Because the septin rod is ~32 nm in length, whereas each subunit itself has a diameter of ~4 nm (Fig. 1A), given the R_0 for the AF555−AF647 pair, FRET should be able to discriminate with adequate resolution interactions between septin subunits situated at different positions within the rod, or the interaction of a septin-interacting protein with septin subunits situated at different positions along the rod, as we have indeed demonstrated is the case (Booth et al., 2015).

$$E = \frac{1}{\left(1 + \frac{r^6}{R_0^6}\right)} = 1 - \frac{F_{DA}}{F_D} \tag{1}$$

For the purposes of using FRET to study protein−protein interactions in vitro, labeling a protein at a single native Cys residue, or a single Cys residue introduced elsewhere by site-directed mutagenesis, with a maleimide derivative of an organic dye has several advantages over use of genetically encoded fluorescent tags (Lam et al., 2012) or incorporation of a nonnatural amino acid side chain that is fluorescent (Wang et al., 2014). Labeling the sulfhydryl group of a solvent accessible Cys in a protein, as was explained previously, is a facile process that can be performed in any laboratory. Additionally, with the rapidly decreasing costs of gene synthesis and seamless cloning techniques, creating engineered single-Cys proteins for expression is very accessible. Furthermore, there is a wide variety of maleimide-derivatized fluorophores available from multiple vendors, allowing for tunability in the system with respect to R_0 or other desired fluorophore attributes. Labeling at Cys with relatively small organic dyes also avoids potential steric clashes that could arise with the considerably bulkier genetically encoded tags, such as GFP, SNAP, CLIP, and Halo, which have to be placed at either one of the termini or within a large solvent-exposed loop (Ishitsuka et al., 2015; Stagge, Mitronova, Belov, Wurm, & Jakobs, 2013). Moreover, the inclusion of a large genetically encoded fluorophore, such as GFP (2.4 × 4.2 nm) (Cody, Prasher, Westler, Prendergast, & Ward, 1993) typically attached via flexible linkers, introduces extra distance and flexibility between the protein of interest and the fluorescent label, potentially affecting results (Ishitsuka et al., 2015). Lastly, bimolecular fluorescence complementation (BiFC) (Kerppola, 2008) and reformation of other bi- or tripartite fluorophores rely on colocalization, do not necessarily give a direct readout of protein−protein interaction, and also form stable, irreversible complexes (Cabantous et al., 2013; Magliery et al., 2005).

Although such techniques do have the ability to capture or trap transient or low-affinity interactions, the formation of stable complexes fails to provide a platform for any mechanistic or dynamic analysis, unlike a FRET-based system that relies only on the kinetic and thermodynamic properties of the interacting proteins themselves.

2. DATA COLLECTION AND ANALYSIS

Once purified septin complexes have been prepared and labeled with fluorophores, careful consideration needs to be given to the subsequent experimental setup and the analysis techniques to be employed. One of the major strengths of spectroscopy is the variety of experiments that can be conducted. For the septins, spectroscopic techniques enable the mechanistic study of polymerization, including elucidation of time constants, dissociation constants, cooperativity, the role of environmental conditions, the effect of ligands (such as GTP or GDP), and the role of septin-binding proteins. We have already demonstrated application of this FRET system to a small subset of possible questions that can be interrogated, specifically demonstrating end-to-end polymerization of Cdc11-capped heterooctamers into filaments, experimental confirmation of apparent K_d (K_d^{app}) for the polymerizing septin system, determining the threshold for the sensitivity of septin filament formation to ionic strength, revealing the inability of Shs1-capped heterooctamers to self-associate end-to-end, but the ability to form heterotypic end-to-end junctions with Cdc11-capped heterooctamers, and showing the interaction of a septin-binding protein (Bni5) (Booth et al., 2015). Here we provide an overview of what needs to be considered for the successful conduct of experiments and data analysis using the spectroscopic FRET-based system we have developed.

2.1 SPECTROSCOPY DATA COLLECTION

Prior to the setup of a spectroscopic experiment, a clear plan is necessary for successful data collection. A successful spectroscopic experiment requires attention to details including sample preparation, data collection, and data analysis. In addition to usual considerations, the septin system has its own idiosyncrasies that need to be addressed.

One of the key considerations with the septin heterooctamer is the ionic strength of the buffer that the final reaction is occurring in and the concentration of the complex. Polymerization of septin rods into higher-order structures is known to be sensitive to the ionic strength of the environment. At low ionic strength (<90 mM salt), Cdc11-capped septin rods self-assemble into paired filaments, whereas at high ionic strength, they remain as individual octamers (Bertin et al., 2008, 2010; Booth et al., 2015). If the objective is to examine interaction of another protein with septin filaments, then care must be taken to keep the ionic strength of the final samples at, conservatively, <50 mM; whereas, if the objective is to determine some feature of

the heterooctamer itself, then the final ionic strength should be at, conservatively, >200 mM. Of course, ionic strength can have other effects that must also be taken into account.

Because of the tendency of lipids to form monolayers and liposomes, which are not compatible with retention of a uniform solution, it must be conceded that standard FRET measurements in a cuvette are not a reliable way to examine the interaction of septins with lipids, even though it is clear that formation of higher-order septin structures from heterooctamers can be strongly influenced on the surface of a membrane mimic (Bertin et al., 2010; Bridges et al., 2014).

If studying septins in their polymerized form, one must use an adequate concentration of heterooctamers (>25 nM in our previously published work) and a sufficient incubation time (~1 h in our previously published work) to allow for their assembly into polymers. Incubation time will be dependent on experimental conditions such as heterooctamer concentration, incubation temperature, viscosity of the buffer, and other experimentally specific factors. To obtain internally self-consistent data when modulating any other experimental variable, the ionic strength should be kept the same across all the samples. For these reasons, it is wise to determine an incubation window in which an experiment could be run consistently and successfully such that the septins are stably assembled, but no deterioration of the system has occurred. For experiments at low ionic strength, it is wise to mix the donor- and acceptor-labeled septin in their high salt storage buffer prior to diluting to decrease ionic strength to ensure equal mixing of the donor- and acceptor-labeled septins. If collecting time-dependent data, similar considerations are necessary and should also include how rapidly the septins self-assemble. For very early time points, the use of other devices, such as a stopped-flow apparatus, may be necessary.

To ensure consistency, the use of master mixes and accurate serial dilutions should be employed. Master mixes and serial dilutions have the added benefit of maintaining consistency between samples and are also useful in preparing standard samples. For FRET studies not only is it important to take careful blanks, but donor-only and acceptor-only standards are also necessary for downstream interpretation of data as described in the following two sections. Lastly, care should be taken in the experimental setup with regard to the fluorimeter to be used and how this specific spectrophotometer is used to collect FRET data (Lakowicz, 2006).

2.2 SEMIQUANTITATIVE SENSITIZED EMISSION

FRET can be determined by measuring the change in acceptor emission at its maximum upon excitation of the donor at its maximum. However, emission of the acceptor will be contaminated by some bleed-through from two sources: some acceptor emission due to acceptor excitation even at the donor excitation wavelength and some tailing of the donor emission into the acceptor emission wavelength (Youvan et al., 1997). Therefore, the apparent FRET of the acceptor needs some correction. To apply such corrections, three measurements are required: $F^{\mathrm{exD,emD}}$, $F^{\mathrm{exA,emA}}$, and $F^{\mathrm{exD,emA}}$, where ex and em refer to excitation and emission,

respectively, and D and A refer to the donor and acceptor, respectively. For example, using AF555 as the donor and AF647 as the acceptor, the excitation and emission maxima are as follows: AF555 (exD: 555 nm, emD: 565 nm) and AF647 (exA: 650 nm, emA 668 nm). FRET between the two requires measurements at exD: 555 nm and emA: 668 nm. The amount of donor bleed-through is determined by a donor-only calibration constant, $x_D = F_D^{exD,emA}/F_D^{exD,emD}$, where D refers to donor-only samples. The x_D value provides a ratiometric calibration constant for removal of the donor bleed-through into the FRET signal. Similarly, $x_A = F_A^{exD,emA}/F_A^{exA,emA}$, where A refers to the acceptor-only samples and provides a correction for the direct acceptor emission by the donor excitation.

$$F_{corr} = F^{exD,emA} - x_D F^{exD,emD} - x_A F^{exA,emA} \quad (2)$$

This treatment allows for the donor bleed-through into the acceptor channel to be corrected (but the much more negligible bleed-through of the acceptor into the donor channel is neglected) (Zeug, Woehler, Neher, & Ponimaskin, 2012). The calibration constants x_A and x_D are fluorophore- and system-dependent and may even vary between experiments. Thus, care needs to be taken to repeat donor-only and acceptor-only measurements routinely. Additionally, the F_{corr} value does not represent a true FRET efficiency, but instead will vary with FRET intensity. Utilization of ratiometric correction factors x_A and x_D, rather than direct subtraction, prevents propagation of errors caused by pipetting (Berney & Danuser, 2003). It is also important to calculate values for x_A for all concentrations used due to the effect of slight changes in the x_A values contributing to much larger changes in the F_{corr} values (Hieb, D'Arcy, Kramer, White, & Luger, 2012). Relative to taking a full emission spectra (including peaks for both the donor and the acceptor), collecting just three data points enables reliable data to be collected rapidly during a time-series and the ability to use such a FRET system in a high-throughput screening mode if a plate reader or other system is available (Hieb et al., 2012; Song, Madahar, & Liao, 2011; Song, Rodgers, Schultz, & Liao, 2012). We successfully employed this three-point data collection method when examining the effect of ionic strength on the K_d^{app} for end-on-end assembly of mixtures of Cdc11-capped rods labeled with donor and acceptor (Booth et al., 2015).

2.3 PRINCIPAL COMPONENT ANALYSIS

Examination of the FRET data can be extended to analysis of collected emission spectra through the application of principal component analysis (PCA). PCA is a widely used and very popular multivariant statistical technique applied in almost all scientific disciplines (Abdi & Williams, 2010). It is an unbiased way to determine what aspect (component) of a system is responsible for the majority of the change (variance) in a system when other parameters are varied. Consistently, PCA has been applied to fluorescence spectra for work done in both chemical and biological systems (Davydov et al., 1995; Frank, Denisov, & Sligar, 2011; Al-Soufi, Novo, Mosquera, & Rodríguez-Prieto, 2011) and, in some cases, with

FRET spectra per se (Davydov et al., 2012). Applications of PCA to fluorescence data occur in two steps. First, the experimental spectra are reduced to their minimal number of "artificial spectra" or principal components which can defined as a linear combination of optimally weighted observed variables which reproduce all the systematic changes in the original experimental spectra. The number of principal components also indicates the number of contributing components or species to the interaction. In the second step, the information from the PCA is used to test different models and find estimates for the model parameters or coefficients. The first step of PCA answers the question of how many species are interacting and the second step enables modeling of the mechanism that provides parameters that best reproduce the spectra (Al-Soufi et al., 2011). Modern programming environments such as Matlab, Python, and SAS make applying PCA to spectra very accessible through use of preprogrammed packages, and there are many excellent sources that go into the mathematical details of applying these techniques (Al-Soufi et al., 2011; Jolliffe, 2002).

An example of how we applied PCA in our system is shown in Fig. 2C–E. In the experiment shown, a fixed concentration (25 nM) of purified Cdc11(E294C)-capped and otherwise Cys-less heterooctamers labeled with AF555 were mixed with increasing concentrations (up to 100 nM) of purified Cdc11(E294C)-capped and otherwise Cys-less heterooctamers labeled with AF647 under polymerizing conditions (45 mM KCl and 50 mM Tris–HCl pH 8.0). As shown in Fig. 2C, there was a clear decrease in the donor emission (555 nm) as the amount of acceptor dye–labeled rods was increased and, as expected for FRET, a corresponding increase in the acceptor emission (668 nm). In Fig. 2D, the known donor-only and acceptor-only spectra for each curve were subtracted out, revealing only the effective FRET spectra, confirming unambiguously the clear decrease in donor emission and concomitant increase in acceptor emission. The insert in Fig. 2D shows that this single principal component—the decrease in donor emission and the increase in acceptor emission—is sufficient to explain the observed spectra, reinforcing the conclusion that a simple 1:1 interaction of the donor and acceptor is occurring. The most parsimonious model (Fig. 2B) to explain this 1:1 interaction would be, of course, that the FRET signal arises from the interaction of a donor dye–labeled Cdc11 with an acceptor dye–labeled Cdc11 at the end-on-end junctions formed as heterooctamers polymerize into filaments. Additionally, because the molar ratio of donor and acceptor fluorophore is known at each concentration, and the donor and acceptor are expected to assemble into septin polymers in a stochastic manner, the ratio of donor and acceptor in a configuration that should yield FRET can be calculated. As seen in Fig. 2E, the values for the predicted curve are in close agreement with the experimentally derived determination of the increased number of donor–acceptor junctions in a configuration productive for FRET. This example shows that, in analyzing the polymerization of septin heterooctamers into filaments, the application of PCA to the FRET spectra readily showed, first, that the FRET signal arose from the formation of end-on-end contacts between a single donor dye–labeled rod and a single acceptor dye–labeled rod and, second, that the

filaments were forming in the expected random stochastic manner expected for a process whose rate-limiting step is the interaction of the ends of the rods.

CONCLUSIONS AND OUTLOOK

Fluorescence spectroscopy provides a versatile platform for gaining insight about the behavior of polymerizing systems in biology. There is a rich history of the utility of such fluorescence methods in the analysis of the more prominent cytoskeletal elements, actin and tubulin. In this article, we demonstrate that the same overall approach can be productively applied to the more enigmatic cytoskeletal polymers derived from the polymerization of heterooctameric septin complexes. We hope that by describing the specific details of the purification and labeling of septin complexes, considerations in the setup of experiments, and the methods we used for data analysis, other investigators will be encouraged to apply this same methodology to address other outstanding questions about septin biology. We presented here two ways that FRET data can be analyzed to provide mechanistic information about septin assembly and interaction with other proteins under a variety of conditions. In addition to the examples shown here, in prior work we have demonstrated the applicability of this FRET system to studying septin assembly under various buffer conditions, using FRET as a spectroscopic ruler, probing the effects of different septin subunits that cap the heterooctameric rods, and studying the specificity of septin-binding proteins (Booth et al., 2015). At this point, we have only just started to see the extent of the information that we, and hopefully others, will be able to derive from application of this FRET method.

ACKNOWLEDGMENTS

This work was supported by NIH R01 grants GM21841 (to JT) and GM101314 (to JT and Berkeley colleague, Prof. Eva Nogales, jointly). The authors especially thank AMGEN Summer Research Scholar Eleanor W. Vane for her assistance in assay development and are grateful to members of the Thorner, Nogales, and Groves Labs for their comments and suggestions during the course of these studies.

REFERENCES

Abdi, H., & Williams, L. J. (2010). Principal component analysis. *WIREs Computational Statistics, 2*, 433–459.

Al-Soufi, W., Novo, M., Mosquera, M., & Rodríguez-Prieto, F. (2011). Principal component global analysis of series of fluorescence spectra. *Reviews in Fluorescence, 2009*, 23–46.

Berney, C., & Danuser, G. (2003). FRET or no FRET: a quantitative comparison. *Biophysical Journal, 84*, 3992–4010.

Bertin, A., McMurray, M. A., Grob, P., Park, S. S., Garcia, G., 3rd, Patanwala, I., … Nogales, E. (2008). *Saccharomyces cerevisiae* septins: supramolecular organization of heterooligomers and the mechanism of filament assembly. *Proceedings of the National Academy of Sciences of the United States of America, 105*, 8274–8279.

Bertin, A., McMurray, M. A., Pierson, J., Thai, L., McDonald, K. L., Zehr, E. A., … Nogales, E. (2012). Three-dimensional ultrastructure of the septin filament network in *Saccharomyces cerevisiae*. *Molecular Biology of the Cell, 23*, 423–432.

Bertin, A., McMurray, M. A., Thai, L., Garcia, G., 3rd, Votin, V., Grob, P., … Nogales, E. (2010). Phosphatidylinositol-4,5-*bis*phosphate promotes budding yeast septin filament assembly and organization. *Journal of Molecular Biology, 404*, 711–731.

Bolanos-Garcia, V. M., & Davies, O. R. (2006). Structural analysis and classification of native proteins from *E. coli* commonly co-purified by immobilised metal affinity chromatography. *Biochimica et Biophysica Acta, 1760*, 1304–1313.

Bonne, D., Heusele, C., Simon, C., & Pantaloni, D. (1985). 4′,6-Diamidino-2-phenylindole, a fluorescent probe for tubulin and microtubules. *The Journal of Biological Chemistry, 280*, 2819–2825.

Booth, E. A., Vane, E. W., Dovala, D., & Thorner, J. (2015). A Foerster resonance energy transfer (FRET)-based system provides insight into the ordered assembly of yeast septin hetero-octamers. *The Journal of Biological Chemistry, 290*, 28388–283401.

Botstein, D., & Fink, G. R. (1988). Yeast: an experimental organism for modern biology. *Science, 240*, 1439–1443.

Botstein, D., & Fink, G. R. (2011). Yeast: an experimental organism for 21st century biology. *Genetics, 189*, 695–704.

Brar, G. A., Yassour, M., Friedman, N., Regev, A., Ingolia, N. T., & Weissman, J. S. (2012). High-resolution view of the yeast meiotic program revealed by ribosome profiling. *Science, 335*, 552–557.

Bridges, A. A., Zhang, H., Mehta, S. B., Occhipinti, P., Tani, T., & Gladfelter, A. S. (2014). Septin assemblies form by diffusion-driven annealing on membranes. *Proceedings of the National Academy of Sciences of the United States of America, 111*, 2146–2151.

Byers, B., & Goetsch, L. (1976). A highly ordered ring of membrane-associated filaments in budding yeast. *The Journal of Cell Biology, 69*, 717–721.

Cabantous, S., Nguyen, H. B., Pedelacq, J.-D., Koraïchi, F., Chaudhary, A., Ganguly, K., … Waldo, G. S. (2013). A new protein-protein interaction sensor based on tripartite split-GFP association. *Science Reports, 3*, 2854.

Carroll, C. W., Altman, R., Schieltz, D., Yates, J. R., & Kellogg, D. (1998). The septins are required for the mitosis-specific activation of the Gin4 kinase. *The Journal of Cell Biology, 143*, 709–717.

Cody, C. W., Prasher, D. C., Westler, W. M., Prendergast, F. G., & Ward, W. W. (1993). Chemical structure of the hexapeptide chromophore of the Aequorea green-fluorescent protein. *Biochemistry, 32*, 1212–1218.

Cooper, J. A., Walker, S. B., & Pollard, T. D. (1983). Pyrene actin: documentation of the validity of a sensitive assay for actin polymerization. *Journal of Muscle Research and Cell Motility, 4*, 253–262.

Davydov, D. R., Deprez, E., Hoa, G. H., Knyushko, T. V., Kuznetsova, G. P., Koen, Y. M., & Archakov, A. I. (1995). High-pressure-induced transitions in microsomal cytochrome P450 2B4 in solution: evidence for conformational inhomogeneity in the oligomers. *Archives of Biochemistry and Biophysics, 320*, 330–344.

Davydov, D. R., Rumfeldt, J. A., Sineva, E. V., Fernando, H., Davydova, N. Y., & Halpert, J. R. (2012). Peripheral ligand-binding site in cytochrome P450 3A4 located with fluorescence resonance energy transfer (FRET). *The Journal of Biological Chemistry, 287*, 6797–6809.

De Virgilio, C., DeMarini, D. J., & Pringle, J. R. (1996). *SPR28*, a sixth member of the septin gene family in *Saccharomyces cerevisiae* that is expressed specifically in sporulating cells. *Nature Reviews. Microbiology, 142*, 2897–2905.

Duong-Ly, K. C., & Gabelli, S. B. (2014). Troubleshooting recombinant protein expression: general. *Methods in Enzymology, 541*, 209–229.

Fares, H., Goetsch, L., & Pringle, J. R. (1996). Identification of a developmentally regulated septin and involvement of the septins in spore formation in *Saccharomyces cerevisiae*. *The Journal of Cell Biology, 132*, 399–411.

Farkasovsky, M., Herter, P., Voss, B., & Wittinghofer, A. (2005). Nucleotide binding and filament assembly of recombinant yeast septin complexes. *Biological Chemistry, 386*, 643–656.

Field, C. M., & Kellogg, D. (1999). Septins: cytoskeletal polymers or signalling GTPases? *Trends in Cell Biology, 9*, 387–394.

Foerster, T. (1946). Energiewanderung und fluoreszenz (energy migration and fluorescence). *Die Naturwissenschaften, 33*, 166–175.

Frank, D. J., Denisov, I. G., & Sligar, S. G. (2011). Analysis of heterotropic cooperativity in cytochrome P450 3A4 using alpha-naphthoflavone and testosterone. *The Journal of Biological Chemistry, 286*, 5540–5545.

Garcia, G., 3rd, Bertin, A., Li, Z., Song, Y., McMurray, M. A., Thorner, J., & Nogales, E. (2011). Subunit-dependent modulation of septin assembly: budding yeast septin Shs1 promotes ring and gauze formation. *The Journal of Cell Biology, 195*, 993–1004.

Garcia, G., 3rd, Finnigan, G. C., Heasley, L. R., Sterling, S. M., Aggarwal, A., Pearson, C. G., … Thorner, J. (2016). Assembly, molecular organization, and membrane-binding properties of development-specific septins. *The Journal of Cell Biology, 212*, 515–529.

Gatzeva-Topalova, P. Z., May, A. P., & Sousa, M. C. (2005). Structure and mechanism of ArnA: conformational change implies ordered dehydrogenase mechanism in key enzyme for polymyxin resistance. *Structure, 13*, 929–942.

Haarer, B. K., & Pringle, J. R. (1987). Immunofluorescence localization of the *Saccharomyces cerevisiae* CDC12 gene product to the vicinity of the 10-nm filaments in the mother-bud neck. *Molecular and Cellular Biology, 7*, 3678–3687.

Hall, P. A., & Russell, S. E. H. (2012). Mammalian septins: dynamic heteromers with roles in cellular morphogenesis and compartmentalization. *The Journal of Pathology, 226*, 287–299.

Hall, P. A., Russell, S. E. H., & Pringle, J. R. (Eds.). (2008). *The septins*. Oxford, UK: Wiley-Blackwell Publishers, Ltd, 370 pp.

Hansen, S. D., Zuchero, J. B., & Mullins, R. D. (2013). Cytoplasmic actin: purification and single molecule assembly assays. *Methods in Molecular Biology (Clifton, NJ), 1046*, 145–170.

Hartwell, L. H. (1971). Genetic control of the cell division cycle in yeast. IV. Genes controlling bud emergence and cytokinesis. *Experimental Cell Research, 69*, 265–276.

Hartwell, L. H., Culotti, J., Pringle, J. R., & Reid, B. J. (1974). Genetic control of the cell division cycle in yeast. *Science, 183*, 46–51.

Hieb, A. R., D'Arcy, S., Kramer, M. A., White, A. E., & Luger, K. (2012). Fluorescence strategies for high-throughput quantification of protein interactions. *Nucleic Acids Research, 40*, e33.1–e33.13.

Ishitsuka, Y., Azadfar, N., Kobitski, A. Y., Nienhaus, K., Johnsson, N., & Nienhaus, G. U. (2015). Evaluation of genetically encoded chemical tags as orthogonal fluorophore labeling tools for single-molecule FRET applications. *The Journal of Physical Chemistry B, 119*, 6611−6619.

Jolliffe, I. T. (2002). *Principal component analysis* (2nd ed.). GmBH, Heidelberg: Springer Verlag, 487 pp.

Kaplan, C., Jing, B., Winterflood, C. M., Bridges, A. A., Occhipinti, P., Schmied, J., … Ewers, H. (2015). Absolute arrangement of subunits in cytoskeletal septin filaments in cells measured by fluorescence microscopy. *Nano Letters, 15*, 3859−3864.

Kerppola, T. K. (2008). Bimolecular fluorescence complementation (BiFC) analysis as a probe of protein interactions in living cells. *Annual Reviews of Biophysics, 37*, 465−487.

Kim, H. B., Haarer, B. K., & Pringle, J. R. (1991). Cellular morphogenesis in the *Saccharomyces cerevisiae* cell cycle: localization of the CDC3 gene product and the timing of events at the budding site. *The Journal of Cell Biology, 112*, 535−544.

Kim, M. S., Froese, C. D., Estey, M. P., & Trimble, W. S. (2011). SEPT9 occupies the terminal positions in septin octamers and mediates polymerization-dependent functions in abscission. *The Journal of Cell Biology, 195*, 815−826.

Kim, Y., Babnigg, G., Jedrzejczak, R., Eschenfeldt, W. H., Li, H., Maltseva, N., … Joachimiak, A. (2011). High-throughput protein purification and quality assessment for crystallization. *Methods: A Companion to Methods in Enzymology. (San Diego, CA), 55*, 12−28.

Knox, R. S. (2012). Foerster's resonance excitation transfer theory: not just a formula. *Journal of Biomedical Optics, 17*, 011003.

Lakowicz, J. R. (2006). *Principles of fluorescence spectroscopy* (3rd ed.). Singapore: Springer, 954 pp.

Lam, A. J., St-Pierre, F., Gong, Y., Marshall, J. D., Cranfill, P. J., Baird, M. A., … Lin, M. Z. (2012). Improving FRET dynamic range with bright green and red fluorescent proteins. *Nature Methods, 9*, 1005−1012.

Macedo, J. N., Valadares, N. F., Marques, I. A., Ferreira, F. M., Damalio, J. C., Pereira, H. M., … Araujo, A. P. (2013). The structure and properties of septin 3: a possible missing link in septin filament formation. *The Biochemical Journal, 450*, 95−105.

Magliery, T. J., Wilson, C. G. M., Pan, W., Mishler, D., Ghosh, I., Hamilton, A. D., & Regan, L. (2005). Detecting protein-protein interactions with a green fluorescent protein fragment reassembly trap: scope and mechanism. *Journal of the American Chemical Society, 127*, 146−157.

McMurray, M. A., & Thorner, J. (2008). Biochemical properties and supramolecular architecture of septin hetero-oligomers and septin filaments. In P. S. Hall, S. E. H. Russell, & J. R. Pringle (Eds.), *The septins* (pp. 49−100). Chichester, West Sussex, UK: Wiley.

Mewes, H. W., Albermann, K., Bähr, M., Frishman, D., Gleissner, A., Hani, J., … Zollner, A. (1997). Overview of the yeast genome. *Nature, 387*(6632 Suppl.), 7−65 [Erratum 387: 737].

Mino, A., Tanaka, K., Kamei, T., Umikawa, M., Fujiwara, T., & Takai, Y. (1998). Shs1p: a novel member of septin that interacts with Spa2p, involved in polarized growth in *Saccharomyces cerevisiae*. *Biochemical and Biophysical Research Communications, 251*, 732−736.

Nishihama, R., Onishi, M., & Pringle, J. R. (2011). New insights into the phylogenetic distribution and evolutionary origins of the septins. *Biological Chemistry, 392*, 681−687.

Ong, K., Wloka, C., Okada, S., Svitkina, T., & Bi, E. (2014). Architecture and dynamic remodelling of the septin cytoskeleton during the cell cycle. *Nature Communications, 81*, 8715−8723.

Ozsarac, N., Bhattacharyya, M., Dawes, I. W., & Clancy, M. J. (1995). The *SPR3* gene encodes a sporulation-specific homologue of the yeast Cdc3/10/11/12 family of bud neck microfilaments and is regulated by AbfI. *Gene, 164*, 157–162.

Pan, F., Malmberg, R. L., & Momany, M. (2007). Analysis of septins across kingdoms reveals orthology and new motifs. *BMC Evolutionary Biology, 7*, 103.101–103.117.

Pietraszewska-Bogiel, A., & Gadella, T. W. (2011). FRET microscopy: from principle to routine technology in cell biology. *Journal of Microscopy, 241*, 111–118.

Renz, C., Johnsson, N., & Gronemeyer, T. (2013). An efficient protocol for the purification and labeling of entire yeast septin rods from *E. coli* for quantitative *in vitro* experimentation. *BMC Biotechnology, 13*, 60.1–60.8.

Robichon, C., Luo, J., Causey, T. B., Benner, J. S., & Samuelson, J. C. (2011). Engineering *Escherichia coli* BL21(DE3) derivative strains to minimize *E. coli* protein contamination after purification by immobilized metal affinity chromatography. *Applied and Environmental Microbiology, 77*, 4634–4646.

Sackett, D. L., Knutson, J. R., & Wolff, J. (1990). Hydrophobic surfaces of tubulin probed by time-resolved and steady-state fluorescence of nile red. *The Journal of Biological Chemistry, 265*, 14899–14906.

Sanders, S. L., & Field, C. M. (1994). Cell division. Septins in common? *Current Biology, 4*, 907–910.

Sellin, M. E., Sandblad, L., Stenmark, S., & Gullberg, M. (2011). Deciphering the rules governing assembly order of mammalian septin complexes. *Molecular Biology of the Cell, 22*, 3152–3164.

Sirajuddin, M., Farkasovsky, M., Hauer, F., Kühlmann, D., Macara, I. G., Weyand, M., … Wittinghofer, A. (2007). Structural insight into filament formation by mammalian septins. *Nature, 449*, 311–315.

Sirajuddin, M., Farkasovsky, M., Zent, E., & Wittinghofer, A. (2009). GTP-induced conformational changes in septins and implications for function. *Proceedings of the National Academy of Sciences of the United States of America, 106*, 16592–16597.

Song, Y., Madahar, V., & Liao, J. (2011). Development of FRET assay into quantitative and high-throughput screening technology platforms for protein-protein interactions. *Annals of Biomedical Engineering, 39*, 1224–1234.

Song, Y., Rodgers, V. G. J., Schultz, J. S., & Liao, J. (2012). Protein interaction affinity determination by quantitative FRET technology. *Biotechnology and Bioengineering, 109*, 2875–2883.

Stagge, F., Mitronova, G. Y., Belov, V. N., Wurm, C. A., & Jakobs, S. (2013). SNAP-, CLIP- and Halo-tag labelling of budding yeast cells. *PLoS One, 8*, e78745.1–e78745.9.

Sun, Y., Wallrabe, H., Seo, S. A., & Periasamy, A. (2011). FRET microscopy in 2010: the legacy of Theodor Förster on the 100th anniversary of his birth. *ChemPhysChem, 12*, 462–474.

de Val, N., McMurray, M. A., Lam, L. H., Hsiung, C. C., Bertin, A., Nogales, E., & Thorner, J. (2013). Native cysteine residues are dispensable for the structure and function of all five yeast mitotic septins. *Proteins, 81*, 1964–1979.

Versele, M., Gullbrand, B., Shulewitz, M. J., Cid, V. J., Bahmanyar, S., Chen, R. E., … Thorner, J. (2004). Protein–protein interactions governing septin heteropentamer assembly and septin filament organization in *Saccharomyces cerevisiae*. *Molecular Biology of the Cell, 15*, 4568–4583.

Wang, K., Sachdeva, A., Cox, D. J., Wilf, N. M., Lang, K., Wallace, S., … Chin, J. W. (2014). Optimized orthogonal translation of unnatural amino acids enables spontaneous protein double-labelling and FRET. *Nature Chemistry, 6*, 393–403 [Erratum 7: 178].

Youvan, D. C., Silva, C. M., Bylina, E. J., Coleman, W. J., Dilworth, M. R., & Yang, M. M. (1997). Calibration of fluorescence resonance energy transfer in microscopy using genetically engineered GFP derivatives on nickel chelating beads. *Biotechnology, 3*, 1–18.

Zent, E., Vetter, I., & Wittinghofer, A. (2011). Structural and biochemical properties of Sept7, a unique septin required for filament formation. *Biological Chemistry, 392*, 791–797.

Zeraik, A. E., Pereira, H. M., Santos, Y. V., Brandão-Neto, J., Spoerner, M., Santos, M. S., … DeMarco, R. (2014). Crystal structure of a *Schistosoma mansoni* septin reveals the phenomenon of strand slippage in septins dependent on the nature of the bound nucleotide. *The Journal of Biological Chemistry, 289*, 7799–7811.

Zeug, A., Woehler, A., Neher, E., & Ponimaskin, E. G. (2012). Quantitative intensity-based FRET approaches - a comparative snapshot. *Biophysical Journal, 103*, 1821–1827.